1521-009X/47/8/794–801$35.00
DRUG METABOLISM AND DISPOSITION

https://doi.org/10.1124/dmd.118.085126
Drug Metab Dispos 47:794–801, August 2019

Enhanced Platelet Response to Clopidogrel in Zucker Diabetic Fatty Rats due to Impaired Clopidogrel Inactivation by Carboxylesterase 1 and Increased Exposure to Active Metabolite[S]

Hongwei Yao, Ruifeng Bai, Tianming Ren, Yani Wang, Jingkai Gu, and Yingjie Guo

School of Life Sciences, Jilin University, Changchun, China

Received November 2, 2018; accepted May 7, 2019

ABSTRACT

Clopidogrel (Clop), a thienopyridine antiplatelet prodrug, is metabolized by cytochrome P450s (CYPs) to an active metabolite, Clop-AM, and hydrolyzed by carboxylesterase (CES)1 to the inactive Clop-acid. Patients with type 2 diabetes (T2DM) tend to have a poor response to Clop due to reduced generation of Clop-AM. Whether a similar response occurs in the Zucker diabetic fatty (ZDF) rat, a commonly used animal model of T2DM, has not been explored. In this work, we compared ZDF and control rats for hepatic CES1- and CYP-mediated Clop metabolism; pharmacokinetics of Clop, Clop-AM, and Clop-acid; and the antiplatelet efficacy of Clop. In contrast to clinical findings, Clop-treated ZDF rats displayed significantly less (50%) maximum platelet aggregation at 4 hours than control rats; the enhanced efficacy was accompanied by higher formation of Clop-AM and lower formation of Clop-acid. In vitro studies showed that hepatic levels of CES1 protein and activity and Ces1e mRNA were significantly lower in ZDF than in control rats, as were the mRNA levels of CYP2B1/2, CYP2C11, and CYP3A2, and levels of CYP2B6-, CYP2C19-, and CYP3A4-related proteins and enzymatic activities in liver microsomes of ZDF rats. Interestingly, liver microsomes of ZDF rats produced higher levels of Clop-AM than that of control rats despite their lower CYP levels, although the addition of fluoride ion, an esterase inhibitor, enhanced Clop-AM formation in control rats more than in ZDF rats. These results suggest that the reduction in CES1-based Clop inactivation indirectly enhances Clop efficacy in ZDF rats by making more Clop available for CYP-mediated Clop-AM formation.

Introduction

Clopidogrel (Clop), a thienopyridine antiplatelet agent, is widely prescribed to prevent thrombotic events in patients with acute coronary syndromes, particularly in those undergoing percutaneous coronary interventions (Yusuf et al., 2001; Wiviott et al., 2007). As a prodrug, Clop requires metabolic biotransformation to a pharmacologically active metabolite, Clop-AM, to prevent platelet aggregation (Savi et al., 2000). It is estimated that about 85% of Clop is rapidly hydrolyzed to an inactive metabolite, clopidogrel acid (Clop-acid), by carboxylesterase (CES)1. The remaining 15% is oxidized by cytochrome P450 (CYP)1A2, CYP2B6, and CYP2C19 to an intermediate metabolite, 2-oxo-Clop, which is further oxidized by CYP2B6, CYP2C9, CYP2C19, and CYP3A4 to Clop-AM (Dansette et al., 2009; Kazui et al., 2010). Clop-AM contains a reactive thiol group that covalently modifies the cysteinyl residues of the platelet $P2Y_{12}$ receptor, leading to prevention of ADP-induced platelet aggregation (Savi et al., 2000). Therefore, the level of Clop-AM and the associated antiplatelet activity is highly dependent on the relative expressions of CES1 and CYPs.

Diabetes is a risk factor for coronary artery disease, cerebrovascular disease, and severe peripheral vascular disease (Luscher et al., 2003), all of which can benefit from the use of Clop. Accumulated evidence points to altered expression and activity of hepatic CYPs and CES in diabetes (Kim and Novak, 2007; Dominguez et al., 2014; Xu et al., 2014; Chen et al., 2015), strongly implicating an interaction between the disease and Clop metabolism. In fact, clinical studies have shown that diabetic patients tend to have a poor response to Clop (Yusuf et al., 2001; Angiolillo et al., 2005, 2007; Brandt et al., 2007; Wiviott et al., 2007) characterized by a lower plasma level of clop-AM and no change in platelet $P2Y_{12}$ receptor function (Erlinge et al., 2008; Angiolillo et al., 2014). However, the role of CYP- and CES1-based Clop metabolism under diabetic conditions has not been investigated.

The Zucker diabetic fatty (ZDF, fa/fa) rat carries a spontaneous mutation of the leptin receptor gene and has been widely used as an animal model of type 2 diabetes mellitus (T2DM). The ZDF rats display symptoms that are commonly encountered in patients with T2DM, such as insulin resistance, high body weight, hyperglycemia, and hyperlipidemia (Shiota and Printz, 2012). They also display changes in the hepatic expression of CYP and conjugation enzymes (Kim and Novak. 2007). In this study, we compared the pharmacokinetics and antiplatelet efficacy of Clop in ZDF and their control rats (Zucker lean, fa/+). In addition, mRNA, protein, and activity of Clop-metabolizing enzymes were measured in an attempt to explain any differences in Clop metabolism in the two strains.

Materials and Methods

Chemicals and Reagents. Clop, Clop-acid, the 3′-methoxyacetophenone derivative of Clop-AM (a stable derivative of Clop-AM), and bifendate

This work was supported by the National Natural Science Foundation of China [Grants 81603182, 81430087, 81673396, 81473142, 31700713, and 81102383].
https://doi.org/10.1124/dmd.118.085126.
[S]This article has supplemental material available at dmd.aspetjournals.org.

ABBREVIATIONS: CES, carboxylesterase; Clop, clopidogrel; Clop-acid, clopidogrel acid; Clop-AM, clopidogrel active metabolite; CYP, cytochrome P450; KF, potassium fluoride; LC-MS/MS, liquid chromatography tandem–mass spectrometry; MPA, maximum platelet aggregation; PNPA, *para*-nitrophenylacetate; T2DM, type 2 diabetes mellitus; ZDF, Zucker diabetic fatty.

TABLE 1

Primer sequences used for quantitative reverse transcription-polymerase chain reaction analysis

Gene	Sequence	Product Length (bp)
Ces1e	Forward: 5′-TCTACCCTACTGGCCTGCAT-3′ Reverse: 5′-CTTCTGGGGCAGAGTCTTGG-3′	124
CYP1A2	Forward: 5′-CCTCACTGAATGGCTTCCACA-3′ Reverse: 5′-TCTCATCATGGTTGACCTGCC-3′	75
CYP2B1/2	Forward: 5′-CTCCTGCAGTTGGACAGAGG-3′ Reverse: 5′-TCCCCGACCAGAGAAATCCT-3′	278
CYP2C11	Forward: 5′-CTGCTGCTGCTGAAACACGTG-3′ Reverse: 5′-GGATGACAGCGTACTATCAC-3′	248
CYP2C22	Forward: 5′-CATGAAGCCCACTGTGGTGCTG-3′ Reverse: 5′-GGAACACAGGCCAGAAGGAAGCT-3′	312
CYP3A2	Forward: 5′-CTAAAGGTTCTGCCACGGGA-3′ Reverse: 5′-CCATGCATCAAGAGCAGTCA-3′	169
GAPDH	Forward: 5′-GGACCAGGTTGTCTCCTGTG-3′ Reverse: 5′-CCATGTAGGCCATGAGGTCC-3′	161

GAPDH, glyceraldehyde-3-phosphate dehydrogenase.

were provided by the Beijing Institute of Pharmacology (Beijing, China). Phenacetin, (S)-mephenytoin, tolbutamide, midazolam, bupropion, acetaminophen, 4-hydroxymephenytoin, α-hydroxymidazolam, hydroxybupropion, and 4-hydroxytolbutamide were purchased form Canspec Scientific & Technology (Shanghai, China). The following chemical reagents (suppliers) were purchased commercially and used as received: NADPH (Gentihold, China); *para*-nitrophenylacetate (PNPA; Aladdin); *p*-nitrophenol (AMEKO, China); phenylmethylsulfonyl fluoride (Solarbio, China); 3′-methoxyphenacyl bromide (TCI, Japan); and potassium fluoride (Aladdin).

Antibodies to rat β-actin and CES1 were purchased from Abcam (Cambridge, MA). Antibodies to human CYP1A2, CYP2B6, CYP2C9, CYP2C19, and CYP3A4 were purchased from Sangon Biotech (Shanghai, China) and, according to the manufacturer, show cross-reactivity with the corresponding rat-related protein.

Animals. Male ZDF and control rats (age 14 weeks, weight 250–300 g) were obtained from Beijing Vital River Laboratory Animal Technology. The controlled animal area was maintained at 22 ± 2°C and 55% ± 10% relative humidity under a 12-hour light/dark cycle (7:00 AM to 7:00 PM). All animal procedures were approved by the Institutional Animal Care and Use Committee of Jilin University.

Assessment of Platelet Aggregation. ADP-induced platelet aggregation was measured in platelet-rich plasma by light transmission aggregometry before the dose and at 4 hours postdose. Briefly, blood was collected in tubes containing sodium citrate (3.8%). Platelet-rich plasma was prepared as a supernatant after centrifugation of citrated blood at 1000 rpm for 5 minutes. Platelet-poor plasma was obtained by centrifugation of the remaining blood at 5000 rpm for 15 minutes. For each measurement, light transmission was adjusted to 0% with platelet-rich plasma and to 100% with platelet-poor plasma. Platelet aggregation in platelet-rich plasma was determined at 37°C during a 5-minute monitoring period after the addition of agonist (5 mM ADP) using a LBY-NJ4A automatic platelet aggregation analyzer (PRECIL, Beijing, China).

Pharmacokinetic Study. Rats were fasted overnight before receiving an oral dose of Clop (75 mg/kg). Serial blood samples were collected into heparinized tubes before the dose and at 0.08, 0.25, 0.5, 0.75, 1, 2, 4, 7, and 10 hours postdose. Plasma was separated immediately by centrifugation at 13,000 rpm for 3 minutes at 4°C.

For determination of Clop-AM, a 50-μl aliquot of plasma was transferred into a sampling tube containing 50 μl internal standard working solution (bifendate 50 ng/ml) and 100 μl 3′-methoxyphenacyl bromide (100 mM) to derivatize sulfhydryl-containing substances to chemically stable compounds. After standing in the dark for 10 minutes, the mixture was vortexed for 1 minute and centrifuged at 13,000 rpm for 5 minutes. The upper layer solution was collected and kept at −80°C pending analysis by liquid chromatography tandem–mass spectrometry (LC-MS/MS).

For determination of Clop and Clop-acid, a 50-μl aliquot of plasma was mixed with 400 μl acetonitrile and 50 μl bifendate working solution to precipitate protein. The mixture was vortexed for 1 minute and centrifuged at 13,000 rpm for 5 minutes, after which the upper layer was collected and stored at −80°C pending analysis by LC-MS/MS.

Determination of Pharmacokinetic Parameters. Noncompartmental pharmacokinetic parameters including C_{max}, the time to C_{max}, area under the plasma concentration–time curve, and terminal half-life were calculated using the software DAS 3.0 (Drug and Statistics Software, Mathematical Pharmacology Professional Committee of China, Shanghai, China).

Quantitative Reverse Transcription-Polymerase Chain Reaction Analysis. Total RNA was extracted from 20 to 30 mg frozen hepatic tissue using a Total RNA Kit (OMEGA, Japan). RNA concentrations were measured using a NanoDrop 1000 Spectrophotometer (Thermo Fisher Scientific, Waltham, MA). Total RNA (1 μg) was reverse-transcribed to cDNA with a reverse-transcriptase Primer Mix using the PrimeScript reverse-transcriptase reagent with genomic DNA Eraser (TaKaRa Biotech, Japan), according to the manufacturer's protocol. Quantitative polymerase chain reaction was performed using gene-specific primers (Table 1) and SYBR Green polymerase chain reaction Master Mix (TaKaRa Biotech) on a LightCycler480 System (Roche, Switzerland). The housekeeping gene glyceraldehyde-3-phosphate dehydrogenase was used as an internal control. The relative quantitation of gene expression was performed using the comparative C_t ($\Delta\Delta C_t$) method (Livak and Schmittgen, 2001).

Liver Microsome Preparation. Liver microsomes were prepared from a homogenate of livers from two rats. Three sets each of microsomes of ZDF and control rats were prepared from homogenates of livers from a total of six rats. Livers were pooled and homogenized in 3-fold volumes of ice-cold buffer containing 0.25 M sucrose, 50 mM Tris-HCl, 1 mM phenylmethylsulfonyl fluoride, and 1 mM EDTA (pH 7.4), followed by centrifugation at 10,000*g* for 20 minutes at 4°C. Supernatants were collected and centrifuged at 100,000*g* for 60 minutes at 4°C. Microsomal pellets were suspended in Tris-HCl buffer (pH 7.4) containing 20% glycerol and stored at −80°C. Protein concentrations were determined using a bicinchoninic acid protein assay kit (Meilune Biotech, China) using bovine serum albumin as standard.

Western Blot Analysis. Liver microsomes (20 μg) were separated on 10% SDS-PAGE and transferred to polyvinylidene difluoride membranes (Millipore, Billerica, MA). Membranes were incubated with anti-CYP1A2, 2B6, 2C9, 2C19, 3A4, CES1, and β-actin antibodies, as previously described (Edwards et al., 2009). Immunoreactive proteins were visualized using the Odyssey Infrared Imaging System (Li-Cor), as described by the manufacturer. Densitometry measurements were made using Odyssey V3.0 (Li-Cor) normalized to β-actin and calculated as the fold-change compared with the control group.

CES Assay. CES activity in liver microsomes was measured spectrophotometrically by hydrolyzing PNPA to *p*-nitrophenol, as described previously (Yang and Yan, 2007). Briefly, 20 μg liver microsomes in 100 mM potassium phosphate buffer (pH 7.4) were incubated with different concentrations of PNPA at 37°C for 5 minutes. The absorbance at 405 nm was recorded with a microplate reader (BioTek, Vermont), and *p*-nitrophenol was determined using a six-point standard curve.

CYP Assays. Rat liver microsomes were incubated with a mixture of the following CYP probe substrates: phenacetin for CYP1A2, bupropion for CYP2B, tolbutamide for CYP2C9-related protein, (S)-mephenytoin for CYP2C19-related protein, and midazolam for CYP3A. The reaction medium contained 100 mM

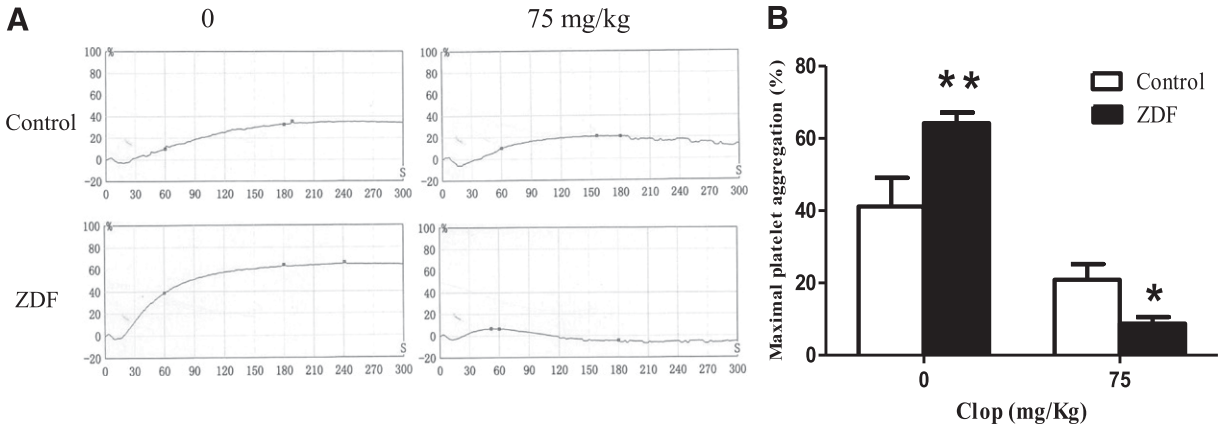

Fig. 1. Effect of Clop on ADP-mediated platelet aggregation in ZDF and control rats. (A) Platelet aggregation–time curves and (B) maximal platelet aggregation in ZDF and control rats 5 minutes before and after administration of a 75 mg/kg oral dose of Clop. Platelet aggregation was determined using a LBY-NJ4A automatic platelet aggregation analyzer after the addition of 5 mM ADP. Data are expressed as mean ± S.D. (n = 6). *$P < 0.05$; **$P < 0.01$ compared with control rats.

potassium phosphate buffer (pH 7.4), 1 mM NADPH, 0.3 mg/ml microsomal protein, and the five probe substrates at final concentrations of 5 and 10 μM for phenacetin, 10 and 20 μM for bupropion, 40 and 80 μM for tolbutamide, 20 and 40 μM for (S)-mephenytoin, and 1.25 and 2.5 μM for midazolam. Incubations were initiated by addition of NADPH and terminated after 20-minute incubation by addition of 150 μl ice-cold methanol containing 50 ng/ml oxcarbazepine (internal standard). Mixtures were centrifuged at 15,000g for 10 minutes at 4°C, after which a 40-μl aliquot of supernatant was injected directly into the LC-MS/MS system to determine the metabolic products (acetaminophen, hydroxybupropion, 4-hydroxytolbutamide, 4-hydroxymephenytoin, and α-hydroxymidazolam).

Clop Metabolism in Liver Microsomes. Incubation mixtures contained 0.6 mg/ml liver microsomes from ZDF and control rats, 1 mM NADPH, 1 mM glutathione, 10 mM magnesium chloride, and Clop at concentrations of 0.75, 1, 1.25, 2.5, and 5 μM. Incubations were performed in the absence and presence of 0.1 M KF (potassium flouoride) in a final volume of 150 μl 100 mM potassium phosphate buffer (pH 7.4). Mixtures were preincubated at 37°C for 5 minutes before reactions were initiated by addition of NADPH. After incubation at 37°C for 100 minutes, 50-μl aliquots of incubation mixtures were collected and treated as described in pharmacokinetic studies. The levels of Clop-AM and Clop-acid were measured by LC-MS/MS.

LC-MS/MS Analysis. The LC-MS/MS system consisted of a Shimadzu LC-20ADXR high-pressure liquid chromatography system (Shimadzu, Japan) coupled to a Qtrap 5500 mass spectrometer (Sciex, Ontario, Canada) equipped with a TurboIonSpray source. Chromatographic separation was achieved on a SUPELCO Ascentis-C18 column (50 × 4.6 mm, 5 μM) (Waters) maintained at 40°C. For Clop-AM, the mobile phase consisted of 0.1% formic acid in water (solvent A) and 0.1% formic acid in acetonitrile (solvent B) delivered at 1 ml/min, according to the following linear gradient: 0–0.3 minute, 45% B; 0.3–1.0 minute, 45%–95% B; 1.0–2.5 minutes, 95% B; 2.5–2.7 minutes, 95%–45% B; and 2.7–4.0 minutes, 45% B. For Clop and Clop-acid, the mobile phase consisted of 3 mM ammonium acetate in water (solvent A) and acetonitrile (solvent B) delivered at 0.8 ml/min, according to the following linear gradient: 0–0.1 minute, 30% B; 0.1–0.6 minute, 30%–90% B; 0.6–1.9 minutes, 90% B; 1.9–2.0 minutes, 90%–30% B; and 2.0–3.0 minutes, 30% B. Details of mass spectrum parameters are listed in Supplemental Table 1.

For simultaneous determination of the five metabolites of CYP probe drugs, the LC-MS/MS system consisted of a Shimadzu high-pressure liquid chromatography SIL-20A XR system (Shimadzu) coupled to QTRAP 4000 mass spectrometer (AB SCIEX) equipped with a TurboIonSpray source. Chromatographic separation was achieved on a ZORBAX SB-C18 column (150 × 4.6 mm, 5 μM) (Agilent) maintained at 40°C. The mobile phase consisted of 0.1% formic acid in water (solvent A) and methanol (solvent B) delivered at 1 ml/min according to the following linear gradient: 0–0.5 minute, 15% B; 0.5–1.8 minutes, 15%–60% B; 1.8–2.5 minutes, 60% B; 2.5–3.0 minutes, 60%–90% B; 3.0–5.0 minutes, 90% B; 5.0–5.2 minutes, 90%–15% B; and 5.2–7.5 minutes, 15% B. Details of mass spectrum parameters are listed in Supplemental Table 1.

Statistical Analysis. All data are presented as mean ± S.D. Significant differences between groups were determined using an unpaired Student's t test. A two-tailed test with $P < 0.05$ was considered to be statistically significant.

Results

Antiplatelet Aggregation Efficacy of Clop. To examine the influence of diabetes on the antiplatelet efficacy of Clop, the maximum platelet aggregation (MPA) in ZDF and control rats before and at 4 hours after administration of a single 75 mg/kg dose of Clop was compared. As shown in Fig. 1, the baseline MPA in response to ADP was significantly higher in ZDF rats than in control rats, indicating that diabetes increases the platelet reactivity to ADP. In contrast, at 4 hours after the dose, the MPA was about 2.0-fold less in ZDF rats than in control rats (8.8% vs. 20.9%, $P < 0.05$), supporting an enhanced antiplatelet efficacy of Clop in ZDF rats.

Pharmacokinetics of Clop and Its Metabolites. As a prodrug, the antiplatelet effect of Clop is mediated by Clop-AM such that variation in its level results in different degrees of inhibition of ADP-induced platelet aggregation. To investigate the enhanced antiplatelet efficacy of Clop, male ZDF and control rats were administered single oral 75 mg/kg doses of Clop, after which blood samples were withdrawn and plasma concentrations of Clop, Clop-AM, and Clop-acid were determined. The time course of the three analytes is shown in Fig. 2, and their pharmacokinetic parameters are summarized in Table 2. The results show that Clop-AM and Clop-acid concentrations are significantly higher and lower, respectively, in ZDF rats than in control rats throughout the 10-hour time course of the study, consistent with the elevated antiplatelet efficacy of Clop in ZDF rats.

CES1 and CYP mRNA Expression in Liver Tissue. Clop-AM concentrations are highly dependent on the relative levels and activities of CES1 and CYPs. To investigate the increased Clop-AM generation in ZDF rats, we first measured hepatic mRNA levels of six rat-specific genes (*Ces1e*, *CYP1A2*, *CYP2B1/2*, *CYP2C22*, *CYP2C11*, and *CYP3A2*), which correspond to their respective human orthologs (*CES1*, *CYP1A2*, *CYP2B6*, *CYP2C9*, *CYP2C19*, and *CYP3A4*). As shown in Fig. 3, the hepatic mRNA levels of *CYP2B1/2*, *CYP2C11*, and *CYP3A2* in ZDF rats are significantly lower (56%, 30%, and 43%, respectively) than their levels in control rats, accompanied by a significantly lower (50%) level of *Ces1e* mRNA. In contrast, the levels of *CYP1A2* and *CYP2C22* mRNA levels were not significantly different in the two groups.

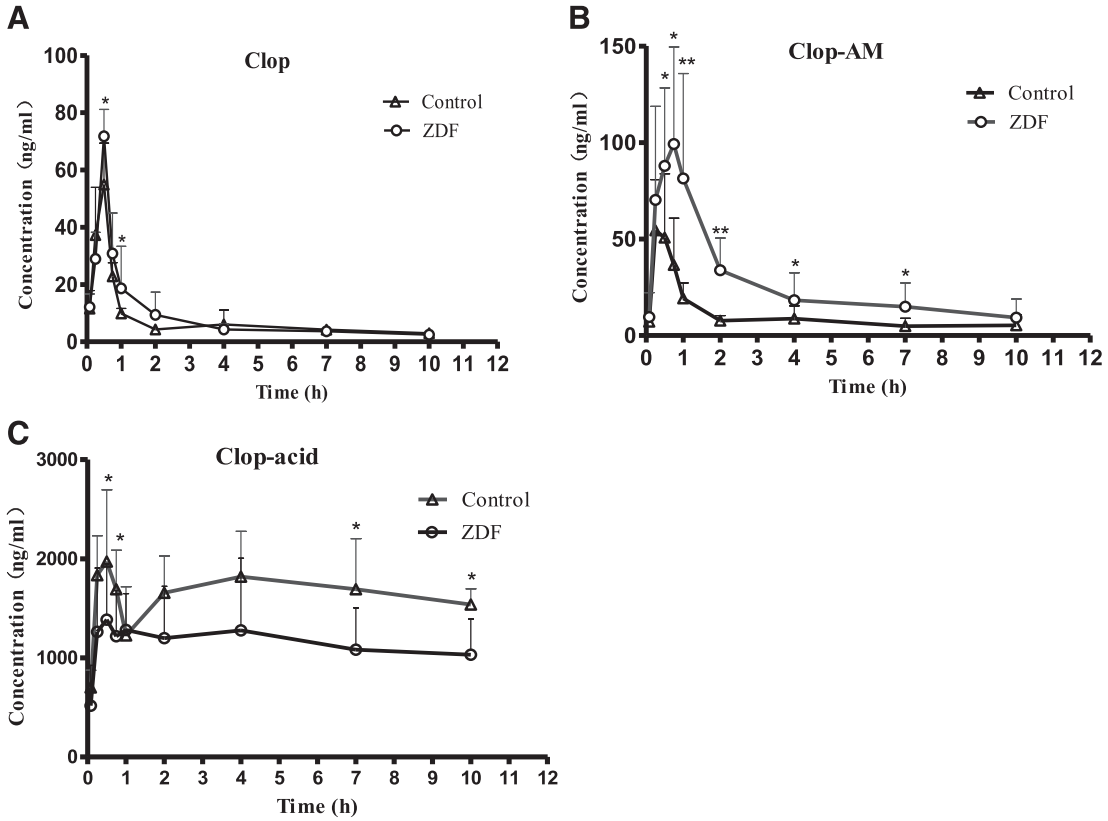

Fig. 2. Plasma concentration–time curves of (A) Clop, (B) Clop-AM, and (C) Clop-acid in ZDF and control rats after single oral 75 mg/kg doses of Clop. Data are mean ± S.D. (n = 6). *$P < 0.05$; **$P < 0.01$ compared with control rats.

CES1 and CYP Protein Levels and Activity in Liver Microsomes. Levels of CES1and CYP proteins in liver microsomes are shown in Fig. 4. CES1, CYP2B6-, CYP2C19-, and CYP3A4-related proteins were significantly lower in ZDF rats than in control rats, but there were no significant differences in CYP1A2- and CYP2C9-related proteins. In terms of activity, the rates of formation of metabolites (Fig. 5) show that the activities of CES, CYP2B, CYP2C19-related protein, and CYP3A are significantly lower in ZDF rats at all substrate concentrations, whereas the activities of CYP1A2- and CYP2C9-related protein are comparable in the two strains. Previous studies have shown that rat CYP2C22 is homologous to human CYP2C8 and CYP2C9 (Qian et al., 2010), and CYP2C11 shows S-mephenytoin 4′-hydroxylase activity (Yasumori et al., 1993). Together with our results, this indicates that the differences in CYP and CES activities in the two strains are consistent with the alterations in the corresponding mRNA and protein levels.

In total, our results demonstrate that the levels and activities of CES1, CYP2B, CYP3A, and CYP2C19 are significantly decreased in ZDF rats, potentially causing an attenuation of Clop metabolism.

Clop Metabolism in Liver Microsomes. Fluoride ion is an inhibitor of esterase activity with adequate potency (Cimasoni, 1966; Krupka, 1966). To explore the contribution of CES1 and CYPs to the formation of Clop-AM, liver microsomes of ZDF and control rats were incubated with different concentrations of Clop for 100 minutes at 37°C in the presence and absence of potassium fluoride. As shown in Fig. 6, Clop is metabolized to significantly lower levels of Clop-acid, but significantly higher levels of Clop-AM in the absence of KF in ZDF rats compared with control rats, consistent with in vivo results. KF almost completely inhibited CES1-based Clop-acid production in both ZDF rats and control rats, and significantly increased the formation of Clop-AM in control rat

TABLE 2

Pharmacokinetic parameters of Clop, Clop-AM, and Clop-acid in ZDF and control rats

Data are mean ± S.D.

Parameter Unit	Clop-AM		Clop-Acid		Clop	
	Control	ZDF	Control	ZDF	Control	ZDF
$AUC_{0\text{-}t}$ ($\mu g \times h/l$)	102.5 ± 11.8	268.9 ± 36.1*	17,224 ± 2900	10,751 ± 3535**	73.8 ± 17.1	84.5 ± 24.4
$AUC_{0\text{-}\infty}$ ($\mu g \times h/l$)	170.7 ± 20.5	308.5 ± 99.3*	54,492 ± 13,827	22,028 ± 8642**	106.9 ± 31.6	126.6 ± 58.0
C_{max} ($\mu g/l$)	58.6 ± 32.4	113.7 ± 49.2**	2862.5 ± 812.9	1678.0 ± 587.5**	61.6 ± 5.4	71.8 ± 9.4
T_{max} (h)	0.4 ± 0.1	0.6 ± 0.1**	3.1 ± 2.5	3.5 ± 3.5	0.45 ± 0.1	0.5 ± 0.1
$t_{1/2}$ (h)	3.8 ± 1.2	3.3 ± 2.9	11.2 ± 17.3	10.5 ± 5.1	7.3 ± 4.7	12.7 ± 6.1

AUC, area under the plasma concentration–time curve; $t_{1/2}$, half-life; T_{max}, time to C_{max}.
*$P < 0.01$; **$P < 0.05$ vs. control rats.

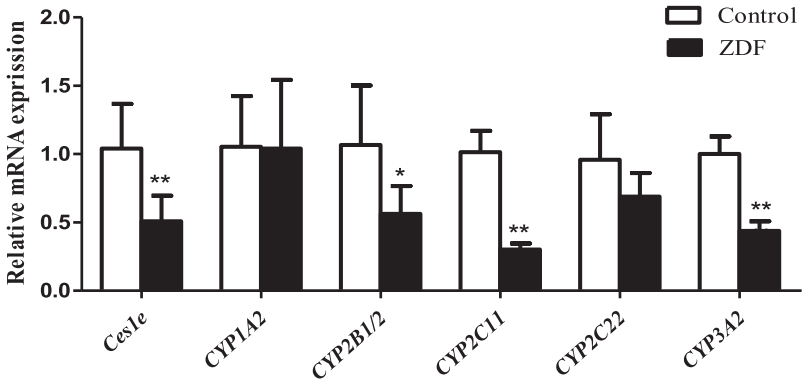

Fig. 3. Ces1e, CYP1A2, CYP2B1/2, CYP2C11, CYP2C22, and CYP3A2 mRNA levels in liver tissues of ZDF and control rats. Data are expressed as mean ± S.D. (n = 6). Values of relative mRNA expression are normalized by the housekeeping gene (glyceraldehyde-3-phosphate dehydrogenase). *$P < 0.05$; **$P < 0.01$ compared with control rats.

microsomes treated with all used concentrations of Clop and in ZDF rat microsomes treated with the two lower concentrations of Clop.

Discussion

A poor response to Clop in patients with T2DM has the potential to be clinically significant (Erlinge et al., 2008; Angiolillo et al., 2014). Whether a similarly poor response occurs in ZDF rats has not been established. We found that both control and ZDF rats were responsive to Clop, but the responsiveness was greater in ZDF rats (Fig. 1). Thus, our results show that, rather than being resistant to Clop, ZDF rats experience a greater antiplatelet effect than control rats.

Platelet reactivity to ADP has been reported to be higher in T2DM patients due to increased $P2Y_{12}$ receptor expression and downstream signaling (Tschoepe et al., 1990; Aronson et al., 1996; Hu et al., 2017). Consistently, we observed higher platelet reactivity to ADP in ZDF rats relative to control rats. However, at 4 hours after Clop administration, ZDF rats displayed lower platelet reactivity to ADP (Fig. 1B) accompanied by higher levels of Clop-AM (Fig. 2B). This result supports the view that the enhanced antiplatelet reactivity to ADP in ZDF rats is the result of increased Clop metabolism to Clop-AM.

As stated previously, the formation of Clop-AM is highly dependent on the relative expression of CES1 and CYPs. Our results show that the levels of CES1 protein (Fig. 4) and *Ces1e* mRNA (Fig. 3) and CES1

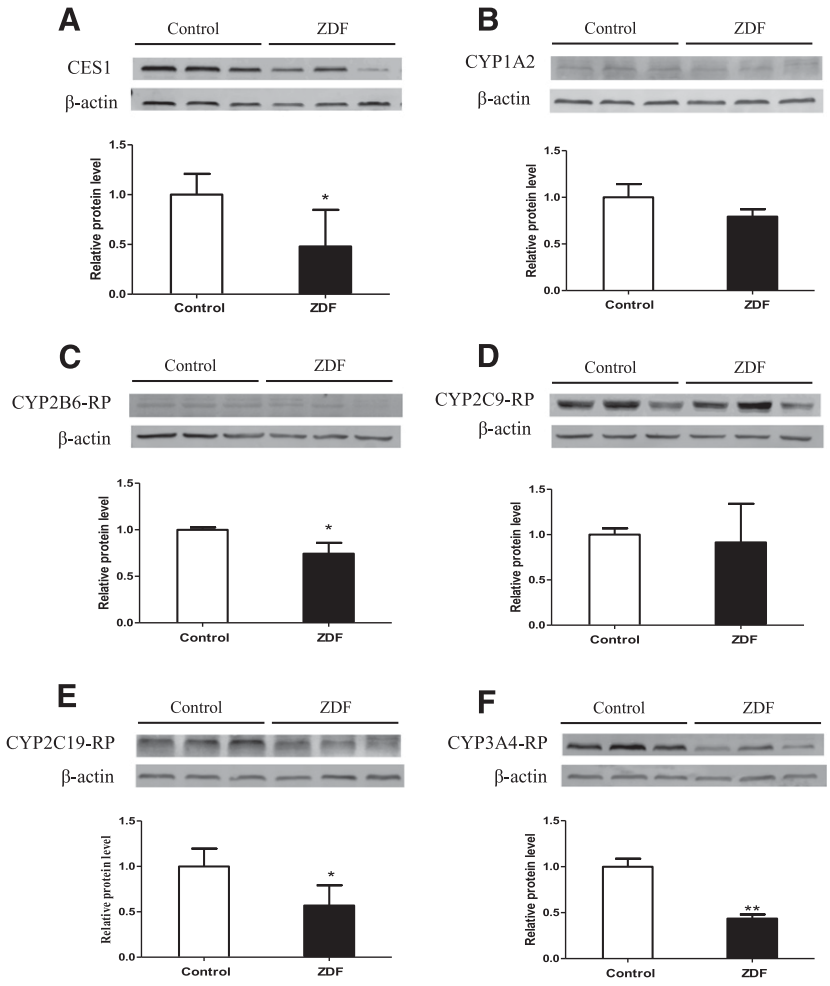

Fig. 4. Hepatic microsomal protein levels of (A) CES1, (B) CYP1A2, (C) CYP2B6-RP, (D) CYP2C9-RP, (E) CYP2C19-RP, and (F) CYP3A4-RP in ZDF and control rats (RP, related protein). Data are expressed as mean ± S.D. (n = 6). Values of relative protein levels are normalized by the housekeeping protein values (β-actin). *$P < 0.05$; **$P < 0.01$ compared with control rats.

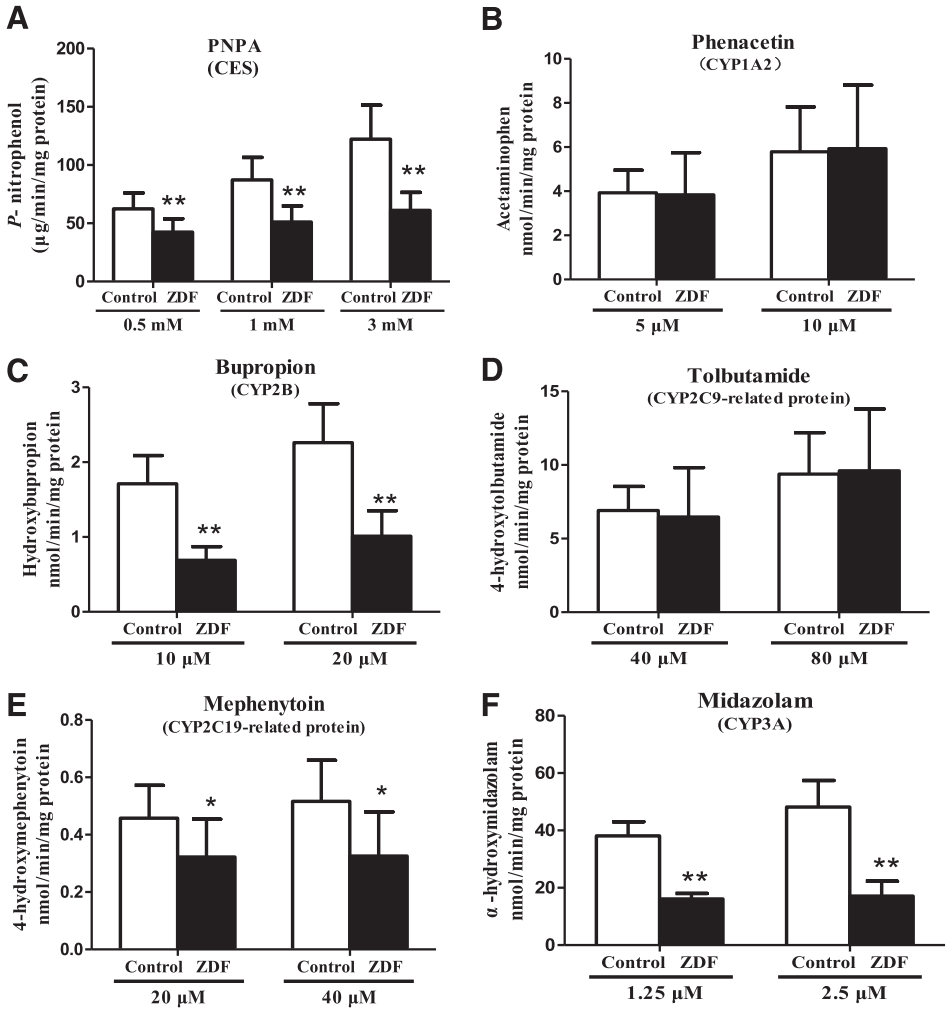

Fig. 5. Hepatic microsomal activities of (A) CES, (B) CYP1A2, (C) CYP2B, (D) CYP2C9-RP, (E) CYP2C19-RP, and (F) CYP3A in ZDF and control rats (RP, related protein). Data are expressed as mean ± S.D. ($n = 6$). *$P < 0.05$; **$P < 0.01$ compared with control rats.

catalytic activity (Fig. 5A) are all significantly lower in ZDF rats than in control rats, which are consistent with the significantly lower area under the plasma concentration–time curve$_{0\text{-t}}$ of Clop-acid (Table 2). Furthermore, functional analyses showed reduced activities of CYP2B, CYP2C19-related protein, and CYP3A in liver microsomes of ZDF rats (Fig. 5), accompanied by attenuation of their corresponding mRNA (Fig. 3) and protein levels. This indicates that the levels of Clop-metabolizing CYP enzymes are also decreased in ZDF rats.

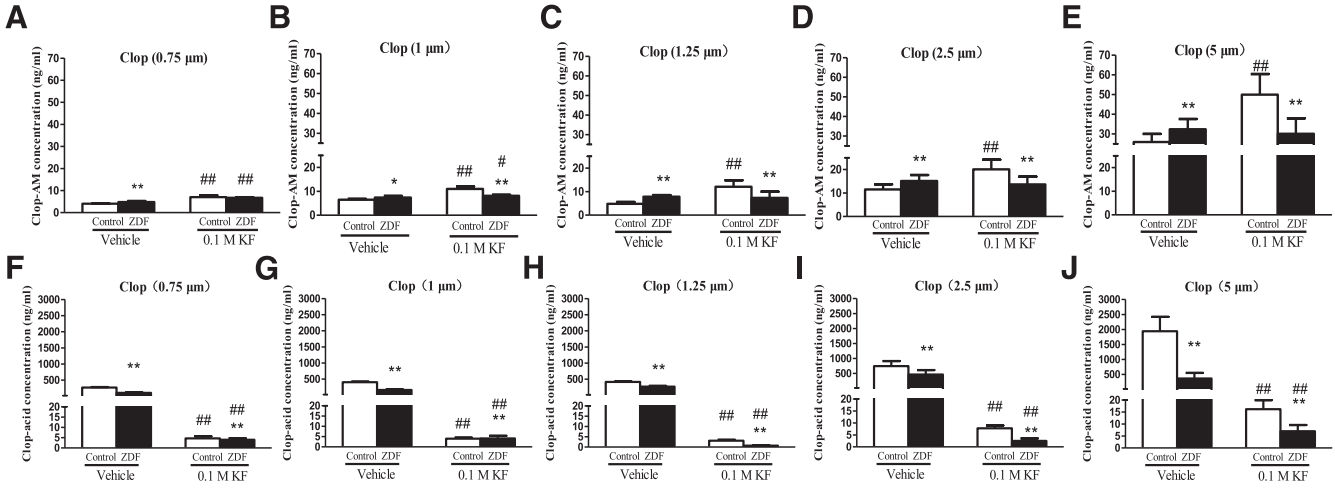

Fig. 6. (A–E) Clop-AM levels and (F–J) Clop-acid levels in liver microsomes of ZDF and control rats incubated with Clop concentrations of (A and F) 0.75, (B and G) 1, (C and H) 1.25, (D and I) 2.5, and (E and J) 5 μM for 100 minutes in the presence or absence of 0.1 M KF. Data are mean ± S.D. ($n = 6$). *$P < 0.05$; **$P < 0.01$ compared with control rats. #$P < 0.05$; ##$P < 0.01$ compared with its corresponding rats.

Interestingly, the greater rate of formation of Clop-AM in ZDF rat microsomes compared with control rat microsomes, seen in the absence of KF, was not seen in the presence of KF (Fig. 6, A–E), a result indicating that the enhanced formation of Clop-AM in the ZDF rats was due to differences in CES1 activity between the two groups. Given the fact that 85% of Clop is metabolized by CES1, it is reasonable that CES1 has a dominant role in determining the rates of Clop disposition, and consequently, also the rates of Clop-AM formation from Clop in liver microsomes. The fact that there was no enhancement in Clop-AM levels at the high concentration of Clop in KF-treated ZDF rat microsomes may be explained by the already decreased CES1 and CYP activities in ZDF rats. The lowered CES1 activity may limit the influence of KF, acting through CES1, on Clop levels, particularly when Clop level is high, in ZDF rats; in contrast, the decreases in CYP activity limit the ability of the microsomes to produce Clop-AM despite KF-mediated decrease in Clop disappearance.

Because CES1 and CYPs competitively metabolize Clop, we infer that the higher rates of Clop-AM formation in ZDF rat liver microsomes were due to an increase in CYP-based metabolism caused by the reduction in CES1-based metabolism. This is consistent with the higher the time to C_{max} of Clop-AM seen in the pharmacokinetic study (Table 2). Clearly, a lower activity of CES1 provides a higher concentration of Clop to undergo oxidation to Clop-AM.

The effect of diabetes on the expression of drug-metabolizing enzymes depends on species, diabetic status, and the animal model employed (Chen et al., 2018). As a consequence, differing results have been obtained in studies of the expression and activity of CYPs in human patients and in ZDF rats. In humans, CYP1A1 expression was elevated in diabetic patients (Matzke et al., 2000), whereas lower expression and activity of CYP3A4 were observed in liver microsomes of diabetic donors compared with nondiabetic donors (Dostalek et al., 2011). In previous studies on the ZDF rat, there were no significant differences in CYP1A protein levels between ZDF and control rats (Park et al., 2016), whereas CYP3A2 expression and activity were lower (Park et al., 2016), consistent with results obtained in the present study.

Species differences have also been observed in the expression and activity of CES1. In humans, CES1 activity was higher in white adipose tissue of obese and T2DM patients (Dominguez et al., 2014), whereas hepatic CES1 expression was increased in diabetic *ob*/*ob* and *db*/*db* mice (Xu et al., 2014). However, Chen et al. (2015) found that the expression and activity of CES1 were lower in the small intestine and liver of streptozotocin-induced diabetic mice than in control mice. Similarly, in the present study, we found that the protein level and catalytic activity of CES1 and the level of *Ces1e* mRNA in the livers of ZDF rats were significantly lower than in control rats.

The ZDF rat is the most widely used animal model of obesity-induced T2DM. ZDF rats develop obesity due to hyperphagia caused by abnormal leptin receptor signaling, with the subsequent appearance of T2DM-like symptoms (Chen et al., 2018). However, in contrast to the ZDF rat, human T2DM is polygenic and multifactorial in nature, and the pathophysiological hallmarks develop over many years. In particular, leptin receptor deficiency is not an important contributor to human T2DM as was in ZDF rats, such that ZDF rats show differences in lipid profile and liver glycogen status from humans (Chen et al., 2018). We speculate that these differences are at least partly responsible for the unique responsiveness to Clop observed in this study in ZDF rats. Interestingly, we have also found decreased Clop-AM levels in high-fat diet and streptozotocin-induced diabetic rats (data not shown), as was found in diabetic patients (Erlinge et al., 2008; Angiolillo et al., 2014). Whether Clop metabolism may be emulated in rats subjected to a high-fat diet and in streptozotocin-induced diabetic rats requires further verification.

Furthermore, T2DM can be associated with insulin resistance, oxidative stress, and inflammation, and, consequently, to altered levels of circulating insulin, reactive oxygen species, and interleukin-1/6. The fact that insulin, reactive oxygen species, and interleukin-1/6 can change the expression of drug-metabolizing enzymes (Chen et al., 2018) implicates them in contributing to the unique alteration of drug-metabolizing enzymes seen in this study.

In conclusion, we have demonstrated that ZDF rats exhibit an enhanced platelet response to Clop compared with control rats due to increased formation of Clop-AM. This occurs because the expression and activity of CES1 are decreased in this rat model of diabetes, promoting an increase in CYP-based metabolism of Clop. Our results indicate that CES1 activity has important pharmacological and toxicological consequences in the clinical use of Clop.

Acknowledgments

We thank Zhiqiong Guo, Yixuan Feng, and Runzhi Li for technical assistance with the animal experiments. We also thank John Paul Fawcett for assistance with the writing of the manuscript.

Authorship Contributions

Participated in research design: Guo, Gu.
Conducted experiments: Yao, Wang.
Contributed new reagents or analytic tools: Bai, Ren.
Performed data analysis: Yao.
Wrote or contributed to the writing of the manuscript: Guo, Yao.

References

Angiolillo DJ, Fernandez-Ortiz A, Bernardo E, Ramírez C, Sabaté M, Jimenez-Quevedo P, Hernández R, Moreno R, Escaned J, Alfonso F, et al. (2005) Platelet function profiles in patients with type 2 diabetes and coronary artery disease on combined aspirin and clopidogrel treatment. *Diabetes* **54**: 2430–2435.

Angiolillo DJ, Jakubowski JA, Ferreiro JL, Tello-Montoliu A, Rollini F, Franchi F, Ueno M, Darlington A, Desai B, Moser BA, et al. (2014) Impaired responsiveness to the platelet P2Y12 receptor antagonist clopidogrel in patients with type 2 diabetes and coronary artery disease. *J Am Coll Cardiol* **64**:1005–1014.

Angiolillo DJ, Shoemaker SB, Desai B, Yuan H, Charlton RK, Bernardo E, Zenni MM, Guzman LA, Bass TA, and Costa MA (2007) Randomized comparison of a high clopidogrel maintenance dose in patients with diabetes mellitus and coronary artery disease: results of the Optimizing Antiplatelet Therapy in Diabetes Mellitus (OPTIMUS) study. *Circulation* **115**:708–716.

Aronson D, Bloomgarden Z, and Rayfield EJ (1996) Potential mechanisms promoting restenosis in diabetic patients. *J Am Coll Cardiol* **27**:528–535.

Brandt JT, Payne CD, Wiviott SD, Weerakkody G, Farid NA, Small DS, Jakubowski JA, Naganuma H, and Winters KJ (2007) A comparison of prasugrel and clopidogrel loading doses on platelet function: magnitude of platelet inhibition is related to active metabolite formation. *Am Heart J* **153**:66.e69-16.

Chen F, Li DY, Zhang B, Sun JY, Sun F, Ji X, Qiu JC, Parker RB, Laizure SC, and Xu J (2018) Alterations of drug-metabolizing enzymes and transporters under diabetic conditions: what is the potential clinical significance? *Drug Metab Rev* **50**:369–397.

Chen R, Wang Y, Ning R, Hu J, Liu W, Xiong J, Wu L, Liu J, Hu G, and Yang J (2015) Decreased carboxylesterases expression and hydrolytic activity in type 2 diabetic mice through Akt/mTOR/HIF-1α/Stra13 pathway. *Xenobiotica* **45**:782–793.

Cimasoni G (1966) Inhibition of cholinesterases by fluoride in vitro. *Biochem J* **99**:133–137.

Dansette PM, Libraire J, Bertho G, and Mansuy D (2009) Metabolic oxidative cleavage of thioesters: evidence for the formation of sulfenic acid intermediates in the bioactivation of the antithrombotic prodrugs ticlopidine and clopidogrel. *Chem Res Toxicol* **22**:369–373.

Dominguez E, Galmozzi A, Chang JW, Hsu KL, Pawlak J, Li W, Godio C, Thomas J, Partida D, Niessen S, et al. (2014) Integrated phenotypic and activity-based profiling links Ces3 to obesity and diabetes. *Nat Chem Biol* **10**:113–121.

Dostalek M, Court MH, Hazarika S, and Akhlaghi F (2011) Diabetes mellitus reduces activity of human UDP-glucuronosyltransferase 2B7 in liver and kidney leading to decreased formation of mycophenolic acid acyl-glucuronide metabolite. *Drug Metab Dispos* **39**:448–455.

Edwards H, Xie C, LaFiura KM, Dombkowski AA, Buck SA, Boerner JL, Taub JW, Matherly LH, and Ge Y (2009) RUNX1 regulates phosphoinositide 3-kinase/AKT pathway: role in chemotherapy sensitivity in acute megakaryocytic leukemia. *Blood* **114**:2744–2752.

Erlinge D, Varenhorst C, Braun OO, James S, Winters KJ, Jakubowski JA, Brandt JT, Sugidachi A, Siegbahn A, and Wallentin L (2008) Patients with poor responsiveness to thienopyridine treatment or with diabetes have lower levels of circulating active metabolite, but their platelets respond normally to active metabolite added ex vivo. *J Am Coll Cardiol* **52**:1968–1977.

Hu L, Chang L, Zhang Y, Zhai L, Zhang S, Qi Z, Yan H, Yan Y, Luo X, Zhang S, et al. (2017) Platelets express activated P2Y12 receptor in patients with diabetes mellitus. *Circulation* **136**: 817–833.

Kazui M, Nishiya Y, Ishizuka T, Hagihara K, Farid NA, Okazaki O, Ikeda T, and Kurihara A (2010) Identification of the human cytochrome P450 enzymes involved in the two oxidative steps in the bioactivation of clopidogrel to its pharmacologically active metabolite. *Drug Metab Dispos* **38**:92–99.

Kim SK and Novak RF (2007) The role of intracellular signaling in insulin-mediated regulation of drug metabolizing enzyme gene and protein expression. *Pharmacol Ther* **113**:88–120.

Krupka RM (1966) Fluoride inhibition of acetylcholinesterase. *Mol Pharmacol* **2**:558–569.
Livak KJ and Schmittgen TD (2001) Analysis of relative gene expression data using real-time quantitative PCR and the 2(-Delta Delta C(T)) method. *Methods* **25**: 402–408.
Lüscher TF, Creager MA, Beckman JA, and Cosentino F (2003) Diabetes and vascular disease: pathophysiology, clinical consequences, and medical therapy: part II. *Circulation* **108**: 1655–1661.
Matzke GR, Frye RF, Early JJ, Straka RJ, and Carson SW (2000) Evaluation of the influence of diabetes mellitus on antipyrine metabolism and CYP1A2 and CYP2D6 activity. *Pharmacotherapy* **20**:182–190.
Park SY, Kim CH, Lee JY, Jeon JS, Kim MJ, Chae SH, Kim HC, Oh SJ, and Kim SK (2016) Hepatic expression of cytochrome P450 in Zucker diabetic fatty rats. *Food Chem Toxicol* **96**: 244–253.
Qian L, Zolfaghari R, and Ross AC (2010) Liver-specific cytochrome P450 CYP2C22 is a direct target of retinoic acid and a retinoic acid-metabolizing enzyme in rat liver. *J Lipid Res* **51**: 1781–1792.
Savi P, Pereillo JM, Uzabiaga MF, Combalbert J, Picard C, Maffrand JP, Pascal M, and Herbert JM (2000) Identification and biological activity of the active metabolite of clopidogrel. *Thromb Haemost* **84**:891–896.
Shiota M and Printz RL (2012) Diabetes in Zucker diabetic fatty rat. *Methods Mol Biol* **933**: 103–123.
Tschoepe D, Roesen P, Kaufmann L, Schauseil S, Kehrel B, Ostermann H, and Gries FA (1990) Evidence for abnormal platelet glycoprotein expression in diabetes mellitus. *Eur J Clin Invest* **20**: 166–170.
Wiviott SD, Braunwald E, McCabe CH, Montalescot G, Ruzyllo W, Gottlieb S, Neumann FJ, Ardissino D, De Servi S, Murphy SA, et al.; TRITON-TIMI 38 Investigators (2007) Prasugrel versus clopidogrel in patients with acute coronary syndromes. *N Engl J Med* **357**:2001–2015.
Xu J, Yin L, Xu Y, Li Y, Zalzala M, Cheng G, and Zhang Y (2014) Hepatic carboxylesterase 1 is induced by glucose and regulates postprandial glucose levels. *PLoS One* **9**:e109663.
Yang J and Yan B (2007) Photochemotherapeutic agent 8-methoxypsoralen induces cytochrome P450 3A4 and carboxylesterase HCE2: evidence on an involvement of the pregnane X receptor. *Toxicol Sci* **95**:13–22.
Yasumori T, Chen L, Nagata K, Yamazoe Y, and Kato R (1993) Species differences in stereoselective metabolism of mephenytoin by cytochrome P450 (CYP2C and CYP3A). *J Pharmacol Exp Ther* **264**:89–94.
Yusuf S, Zhao F, Mehta SR, Chrolavicius S, Tognoni G, and Fox KK; Clopidogrel in Unstable Angina to Prevent Recurrent Events Trial Investigators (2001) Effects of clopidogrel in addition to aspirin in patients with acute coronary syndromes without ST-segment elevation [published correction appears in *N Engl J Med* (2001) 345:1506; *N Engl J Med* (2001) 345:1716]. *N Engl J Med* **345**:494–502.

Address correspondence to: Dr. Jingkai Gu, School of Life Sciences, Jilin University, Changchun 130012, China. E-mail: gujk@jlu.edu.cn; or Dr. Yingjie Guo, School of Life Sciences, Jilin University, Changchun 130012, China. E-mail: guoyingjie@jlu.edu.cn